Atmos. Meas. Tech. Discuss., https://doi.org/10.5194/amt-2017-340
Manuscript under review for journal Atmos. Meas. Tech.
Discussion started: 20 September 2017

Atmospheric Measurement Techniques Discussions

Minimum Aerosol Layer Detection Sensitivities and their Subsequent Impacts on Aerosol Optical Thickness Retrievals in CALIPSO Level 2 Data Products

Travis D. Toth[1], James R. Campbell[2], Jeffrey S. Reid[2], Jason L. Tackett[3], Mark A. Vaughan[4], Jianglong Zhang[1], and Jared W. Marquis[1]

[1]Dept. of Atmospheric Sciences, University of North Dakota, Grand Forks, ND, USA
[2]Aerosol and Radiation Sciences Section, Marine Meteorology Division, Naval Research Laboratory, Monterey, CA, USA
[3]Science Systems and Applications, Inc., Hampton, VA, USA
[4]NASA Langley Research Center, Hampton, VA, USA

Correspondence to: Travis D. Toth (travis.toth@und.edu)

Abstract.

Due to instrument sensitivities and algorithm detection limits, Level 2 (L2) Cloud-Aerosol Lidar with Orthogonal Polarization (CALIOP) 532 nm aerosol extinction profile retrievals are often populated with retrieval fill values (RFVs), which indicate the absence of detectable levels of aerosol within the profile. In this study, using four years (2007-2008 and 2010-2011) of CALIOP Version 3 L2 aerosol data, the occurrence frequency of daytime CALIOP profiles containing all RFVs (all-RFV profiles) is studied. In the CALIOP data products, the aerosol optical thickness (AOT) of any all-RFV profile is reported as being zero, which may introduce a bias in CALIOP-based AOT climatologies. For this study, we derive revised estimates of AOT for all-RFV profiles using collocated Moderate Resolution Imaging Spectroradiometer (MODIS) Dark Target

Atmos. Meas. Tech. Discuss., https://doi.org/10.5194/amt-2017-340
Manuscript under review for journal Atmos. Meas. Tech.
Discussion started: 20 September 2017

Atmospheric Measurement Techniques Discussions

(DT) and, where available, Aerosol Robotic Network (AERONET) data. Globally, all-RFV profiles comprise roughly 71% of all daytime CALIOP L2 aerosol profiles (i.e., including completely attenuated profiles), accounting for nearly half (45%) of all daytime cloud-free L2 aerosol profiles. The mean collocated MODIS DT (AERONET) 550 nm AOT is found to be near 0.06 (0.08) for CALIOP all-RFV profiles. We further estimate a global mean aerosol extinction profile, a so-called "noise floor", for CALIOP all-RFV profiles. The global mean CALIOP AOT is then recomputed by replacing RFV values with the derived noise floor values for both all-RFV and non-all-RFV profiles. This process yields an improvement in the agreement of CALIOP and MODIS over-ocean AOT.

1 Introduction and Motivation

Cloud-Aerosol Lidar with Orthogonal Polarization (CALIOP) measurements provide critical information on aerosol vertical distribution for studies involving aerosol modeling (e.g., Campbell et al., 2010; Sekiyama et al., 2010; Yu et al., 2010; Zhang et al., 2011; 2014), air quality (e.g., Martin, 2008; Prados et al., 2010; Toth et al., 2014), and aerosol climatic effects (e.g., Huang et al., 2007; Chand et al., 2009; Thorsen and Fu, 2015; Alfaro-Contreras et al., 2016; Toth et al., 2016). In addition, the column-integrated aerosol optical thickness (AOT) derived from Level 2 (L2) CALIOP 532 nm observations is also widely used, in comparing and combining with passive-based L2 aerosol retrievals, for a comprehensive understanding of regional and global aerosol optical properties (e.g., Redemann et al., 2012). Two such passive-based systems are Aqua Moderate Resolution Imaging Spectroradiometer (MODIS), due to its proximity to CALIOP in the "A-Train"

Atmos. Meas. Tech. Discuss., https://doi.org/10.5194/amt-2017-340
Manuscript under review for journal Atmos. Meas. Tech.
Discussion started: 20 September 2017

Atmospheric Measurement Techniques Discussions

satellite constellation (Levy et al., 2013), and Aerosol Robotic Network (AERONET) sun photometers, which is the primary means for validation of satellite AOT retrievals (Holben et al., 1998).

It is well-documented that a discrepancy exists between CALIOP-derived AOTs and those from MODIS data (i.e., CALIOP retrievals lower than MODIS counterparts), albeit invoking varying quality-assurance (QA)/quality control (QC) procedures across different timeframes and spatial domains (e.g., Kacenelenbogen et al., 2011; Kittaka et al., 2011; Redemann et al., 2012; Kim et al., 2013; Ma et al., 2013). These studies tend to attribute the AOT differences to either uncertainties/cloud contamination in the MODIS retrieval, or incorrect selection of the lidar ratio (extinction-to-backscatter ratio; Campbell et al., 2013) when deriving CALIOP aerosol extinction, and subsequent AOT. In a similar fashion, CALIOP AOTs have been evaluated against AERONET-derived AOTs, with the disparities (CALIOP lower) attributed to incorrect CALIOP lidar ratio assumptions, cloud contamination, and differences in instrument viewing angles (Schuster et al., 2012; Omar et al., 2013).

While some studies cite the failure to detect tenuous aerosol layers as a possible factor in the aforementioned AOT discrepancy (Kacenelenbogen et al., 2011; Rogers et al., 2014), the extent to which these layer detection failures contribute to the AOT differences between multiple sensors has not been fully quantified. For L2 CALIOP profiles, an extinction coefficient retrieval is performed only for those range bins where aerosol backscatter is detected above the algorithm noise floor. Otherwise, the bins are assigned fill values (retrieval fill values, or RFVs) within the corresponding profile (i.e., -9999.00s; Vaughan et al., 2009; Winker et al., 2013). In fact, all L2 CALIOP extinction

Atmos. Meas. Tech. Discuss., https://doi.org/10.5194/amt-2017-340
Manuscript under review for journal Atmos. Meas. Tech.
Discussion started: 20 September 2017

Atmospheric Measurement Techniques Discussions

77 profiles contain a non-zero percentage of RFVs. It is thus critical to recognize that since
78 lidar-derived AOTs reflect the integration of range-resolved extinction retrievals, in the
79 absence of multi-spectral instruments (i.e., Raman and high spectral resolution lidars
80 [HSRLs]), there will always be range bins where aerosol is present below the detection
81 thresholds of the instrument. Indeed, even in relatively "clean conditions", low
82 extinction but geometrically deep aerosol loadings can integrate to significant AOT
83 contributions (Reid et al., 2017).

84 For a fairly large subset of CALIOP daytime measurements, no aerosol is
85 detected anywhere within a column and hence no aerosol extinction retrieved. This
86 results in an aerosol extinction profile consisting entirely of RFVs (defined as CALIOP
87 all-RFV profiles in this study). Assigning aerosol extinction coefficients to 0.0 km^{-1} to
88 replace fill values during integration of the extinction coefficient profile results in a
89 corresponding column AOT equal to zero. Note that this scenario further includes those
90 profiles reduced to fill values in the process of applying QA procedures on a per-bin basis
91 (e.g., Campbell et al., 2012; Winker et al., 2013). Thus, it is plausible that a column
92 exhibiting significant AOT may be underestimated in those cases where the aerosol
93 backscatter is both highly diffuse and unusually deep, and thus consistently falls below
94 the algorithm detection threshold.

95 The RFV issue is essentially a layer detectability problem, which has been
96 previously investigated in regional validation studies. For example, Rogers et al. (2014)
97 evaluated CALIOP layer and total-column AOT with the use of collocated HSRL data.
98 Minimum detection thresholds for aerosol extinction were estimated as 0.012 km^{-1} at
99 night and 0.067 km^{-1} during daytime (in a layer median context). From a column-

integrated perspective, CALIOP algorithms were found to underestimate AOT by about 0.02 during nighttime (attributed to tenuous aerosol layers in the free troposphere). During daytime, due to the influence of the solar background signal, CALIOP algorithms were unable to detect about half of weak (AOT < 0.1) aerosol profiles.

At first glance, the RFV issue may seem superfluous, and one easily resolved in a subsequent study. In fact, the issue has already caused some confusion within the literature. For example, some studies (e.g., Redemann et al., 2012; Kim et al., 2013; and Winker et al., 2013) include all-RFV profiles (i.e., AOT = 0) for analysis when evaluating climatological AOT characteristics. Campbell et al. (2012; 2013) and Toth et al. (2013; 2016), on the other hand, do not include all-RFV profiles while generating climatological averages. Clearly, the first approach introduces an artificial underestimation of mean AOT by including profiles where AOT was not retrieved. The latter, however, presumably leads to an overestimation, since its believed likeliest that all-RFV profiles reflect relatively low AOT cases (i.e., lower than any apparent mean sample value) where CALIOP layer detection exhibits a lack of sensitivity to diffuse aerosol presence that caused nothing to be reported within the column. As a result, Kim et al. (2013) and Winker et al. (2013) report global mean CALIOP AOTs lower than those from Campbell et al. (2012) that does not include the profiles. Other factors (e.g., different temporal domains and QA metrics invoked) also contribute to the observed disparity in these global mean AOT computations. This state of affairs indicates a clear need to carefully quantify the occurrence frequency of all-RFV profiles on a global scale, and, if possible, derive representative column-integrated AOT values for RFV profiles.

Atmos. Meas. Tech. Discuss., https://doi.org/10.5194/amt-2017-340
Manuscript under review for journal Atmos. Meas. Tech.
Discussion started: 20 September 2017

122 Further, and as introduced above, for non-all-RFV profiles there remain range
123 bins with RFVs where low aerosol extinction is likely present (the sum of which,
124 however, can result in a relatively significant AOT). Though some QA can filter obvious
125 cases of attenuation-limited profiles (e.g., require aerosol presence within 250 m of the
126 surface as in Campbell et al., 2012; 2013), the only current remedy otherwise is to accept
127 RFV bins as equal to zero extinction, then integrating to obtain a column AOT estimate.
128 It is compelling to investigate, in a manner similar to Rogers et al. (2014), what this
129 quantitative effect is for climatological analysis.
130 In this paper, using four years (2007-2008 and 2010-2011) of daytime
131 observations from CALIOP, Aqua MODIS, and AERONET, we investigate the RFV
132 issue with an emphasis on the following questions:
133 (1) What is the frequency of occurrence of all-RFV profiles in the daytime cloud-free
134 CALIOP data set?
135 (2) By collocating MODIS and AERONET AOTs with CALIOP cloud-free all-RFV
136 profiles, what is the modal AOT associated with this phenomenon and how
137 randomly are the data distributed as a function of passive-derived AOT?
138 (3) What is the quantitative underestimation in CALIOP AOT due to RFVs in profiles
139 where extinction is retrieved?
140 (4) How much of the discrepancy between MODIS and CALIOP L2 over-ocean AOT
141 retrievals can be explained by RFVs and all-RFV profiles?
142 We note that the primary CALIOP laser failed in March 2009, forcing the Cloud-Aerosol
143 Lidar and Infrared Pathfinder Satellite Observations (CALIPSO) mission team to switch
144 to a secondary laser. Therefore, two years of CALIOP aerosol data are analyzed prior to

(2007-2008) and after (2010-2011) the switch to investigate any discernible difference in RFV statistics between the two lidar profiles.

2 Datasets

2.1 CALIOP

Orbiting aboard the CALIPSO satellite within the "A-Train" constellation (Stephens et al., 2002), CALIOP is a two-wavelength (532 and 1064 nm) polarization-sensitive (at 532 nm) elastic backscatter lidar, observing the vertical distribution of aerosols and clouds in Earth's atmosphere since June 2006 (Winker et al., 2010). The 532 nm backscatter profiles measured by CALIOP are used to detect aerosol and cloud features and then retrieve corresponding particle extinction and subsequent AOTs (i.e., column-integrated extinction; Young and Vaughan, 2009) within layer boundaries determined by a multi-resolution layer detection scheme (Vaughan et al., 2009) and the assumption of a lidar ratio based upon aerosol or cloud type (Omar et al., 2005; 2009). For this study, 532 nm aerosol extinction coefficient data from the Version 3 (V3) CALIPSO L2 5 km Aerosol Profile (L2_05kmAProf) product are utilized (Winker et al., 2009; hereafter, all references to CALIOP data imply the 532 nm channel/product). These aerosol profiles are reported in 5 km segments and feature a vertical resolution of 60 m below an altitude of 20.2 km above mean sea level (AMSL). Only CALIOP data collected during daytime conditions are considered for this study, such that comparison with aerosol observations from MODIS and AERONET can be accomplished.

Prior to analysis, advanced QA procedures are performed on the L2_05kmAProf product. This QA scheme is similar to that employed in Campbell et al. (2012) and

168 Winker et al. (2013), detailed descriptions of which are also outlined in our most recent
169 CALIOP-based study (Toth et al., 2016). Extinction retrievals reported in the CALIOP
170 data products that do not pass the full suite of QA tests are converted to RFVs. To limit
171 the influence of clouds on our analysis (i.e., in order to ensure that the RFV issue is
172 occurring due to layer detection sensitivity and not because of attenuation effects caused
173 by cloud presence), each aerosol profile is cloud-screened using the Atmospheric Volume
174 Description (AVD) parameter. We implement the strictest cloud-screening possible, as
175 profiles are flagged "cloudy" if any of the bins within the CALIOP column are classified
176 as cloud.
177
178 **2.2 Aqua MODIS**
179 As an integral part of the payloads for NASA's Terra and Aqua satellites, MODIS is a
180 36 channel spectroradiometer with wavelengths ranging from 0.41 microns to 15 microns.
181 Seven of these channels (0.47-2.13 microns) are used to retrieve aerosol optical
182 properties, such as AOT (e.g., Levy et al., 2013). MODIS L2 aerosol products are
183 reported at a spatial resolution of 10 x 10 km^2 at nadir, with a reported over-ocean
184 expected error of (-0.02*AOT - 10%), (+0.04*AOT + 10%) (Levy et al., 2013).
185 However, uncertainties for individual retrievals may be larger (Shi et al., 2011). In this
186 study, the Effective_Optical_Depth_Best_Ocean (550 nm) parameter in the L2 Collection
187 6 (C6) Aqua MODIS aerosol product (MYD04_L2; Levy et al., 2013) is utilized. Only
188 those retrievals flagged as "Good" and "Very Good" are considered for analysis, as
189 determined by the Quality_Assurance_Ocean parameter within the MYD04_L2 files.
190

Atmos. Meas. Tech. Discuss., https://doi.org/10.5194/amt-2017-340
Manuscript under review for journal Atmos. Meas. Tech.
Discussion started: 20 September 2017

Atmospheric Measurement Techniques Discussions

2.3 AERONET

Developed for the purpose of furthering aerosol research and validating satellite retrievals, NASA's AERONET program is a federated worldwide system of ground-based sun photometers that collect measurements of aerosol optical and radiative properties (Holben et al., 1998). With a reported uncertainty of ± 0.01 – 0.02 (although this estimate is low in the presence of unscreened cirrus clouds; e.g., Chew et al., 2011), AOTs are derived at several wavelengths ranging from 340 nm to 1640 nm. Due to the lack of retrievals at the CALIOP wavelength, AOTs at 532 nm are computed from interpolation of those derived at the 500 and 675 nm channels using an Angstrom relationship (e.g., Shi et al., 2011; Toth et al., 2013). The highest quality V2.0 AERONET data (Level 2.0) are used in this study, as these are both cloud-screened and quality-assured. Also, only observations from coastal/island AERONET sites are considered for comparison with over-ocean CALIOP profiles, despite the potential overestimation of CALIOP AOT in coastal regions due to the CALIPSO aerosol typing algorithms (e.g., Kanitz et al., 2014).

3 Results and Discussion

3.1 Demonstrating how CALIOP backscatter distribution can render profiles of all RFVs

To demonstrate the nature of the RFV problem, Fig. 1 shows an example of cloud free all-RFV CALIOP profiles embedded within curtain plots of total attenuated backscatter (TAB; Fig. 1a) and matching vertical feature mask (VFM; Fig. 1b). Both plots were obtained from the CALIPSO Browse Images website [https://www-calipso.larc.nasa.gov/products/lidar/browse_images/production/], and the data were

Atmos. Meas. Tech. Discuss., https://doi.org/10.5194/amt-2017-340
Manuscript under review for journal Atmos. Meas. Tech.
Discussion started: 20 September 2017

collected from CALIOP during daytime on July 2nd, 2010 over the Arctic. The VFM shows that the range bins within the white box are classified as either surface or clear air features, and thus the corresponding L2 aerosol extinction coefficient profiles (not shown) are all-RFVs (i.e., the AOT=0 scenario).

However, even under pristine conditions, aerosol particles are still present in the atmosphere. For example, the baseline maritime AOT is estimated to be 0.06 ± 0.01 (Kaufman et al., 2005; Smirnov et al., 2011). Thus, aerosol particles are likely present and yet undetected for the all-RFV cases shown in Fig. 1. Similar issues can also exist for profiles for which some aerosol is detected. This scenario is represented by the white arrow in the TAB and VFM plots, and the associated L2 aerosol extinction coefficient profile is depicted in Fig. 1c. An aerosol layer is evident from about 1.5 to 2.5 km AMSL, leaving the remainder of the column as RFVs.

To further demonstrate the RFV phenomenon in the CALIOP dataset, we next examine differences in TAB found in profiles where all-RFV were reported and those where some extinction was retrieved. The CALIPSO Lidar Level 1.5 data product (L1.5) is specifically leveraged for this task, as TAB for the all-RFVs class of data is not included in L2 datasets. The L1.5 product is a merging of the L1 and L2 products, cloud-cleared, screened for non-aerosol features (e.g., surface, subsurface, totally attenuated, invalid, etc.), and available at 20 km (horizontal) and 60 m (vertical) resolutions (Vaughan et al., 2011). One month (February 2008) of daytime L1.5 TAB profiles over all global oceans were collocated with CALIOP AOTs derived from the L2_05kmAProf product. The data was limited to only those L1.5 averages that contain either four contiguous 5 km L2 all-RFV profiles, or, conversely, four contiguous profiles where

Atmos. Meas. Tech. Discuss., https://doi.org/10.5194/amt-2017-340
Manuscript under review for journal Atmos. Meas. Tech.
Discussion started: 20 September 2017

240 extinction was retrieved in each. The selected TAB profiles were then averaged to a 20
241 km resolution for each altitude range (i.e., to obtain over global ocean mean TAB
242 profiles).

243 The results of this analysis are shown in Fig. 2. Profiles of mean TAB over global
244 oceans for February 2008 are shown in Fig. 2a; blue lines show all-RFV profiles and red
245 lines show those where some extinction was retrieved (i.e., non-all-RFVs). For most of
246 the troposphere, little difference is observed between the two profiles (i.e., "clear sky" in
247 the aggregate). However, the profiles begin to deviate below 3 km AMSL, as larger TAB
248 are found for the extinction-retrieved sample (peak TAB is ~0.0031 km^{-1} sr^{-1}) compared
249 to those profiles consisting of all-RFVs (peak TAB value is ~0.0017 km^{-1} sr^{-1}). An
250 additional analysis was conducted (not shown) using data over the Pacific Ocean to check
251 for influences of geographic sampling (i.e., aerosol distribution) on the mean TAB
252 profiles. Both the all-RFV and non-all-RFV mean TAB profiles increase at similar
253 magnitudes after implementing this restriction, thus resulting in only a minor difference
254 between the profiles.

255 Figure 2c shows a second pair of mean TAB profiles, but now restricted to only
256 those L2 CALIOP profiles collocated with MODIS AOTs (collocation process described
257 in Sec. 3.3) between 0.03 and 0.07. Whereas below, the modal MODIS AOT for passive
258 retrievals collocated with all-RFV CALIOP profiles is about 0.05 (see Sect. 3.3 for
259 rationale), this restriction is meant to investigate a more nuanced question. The presence
260 of all-RFV profiles is the result of several processes that can work either independently or
261 in tandem. The dominant cause is, as described above, detection failure. RFVs also
262 occur when the cloud-aerosol discrimination algorithm mistakenly classifies an aerosol

Atmos. Meas. Tech. Discuss., https://doi.org/10.5194/amt-2017-340
Manuscript under review for journal Atmos. Meas. Tech.
Discussion started: 20 September 2017

Atmospheric Measurement Techniques Discussions

263 layer as a cloud, and again when the extinction coefficients retrieved for a detected
264 aerosol layer fail any of the QA metrics (e.g., an out-of-range extinction QC flag). This
265 restriction is meant to limit the influence of layer misclassifications and occasional QA
266 failures, and in particular relatively high AOT cases where unusually high TAB could
267 influence the mean profile. Including such samples would degrade the accuracy of the
268 TAB noise floor estimate that we will use in subsequent analyses described in Sec. 3.5.
269 Relatively speaking, though, the profiles in Fig. 2c are fairly similar to those of Fig. 2a.
270 However, the relative deviation between the two samples now occurs below 2 km AMSL,
271 and the peak value of TAB for non-all-RFVs lowers to around 0.0025 km^{-1} sr^{-1}
272 (illustrating the effect of the MODIS AOT restriction). Also, for context, we include
273 corresponding profiles of attenuated scattering ratio (TAB/molecular attenuated
274 backscatter) for both analyses in Figs. 2b and 2d.

275 The initial point of this comparison is that the mean TAB for all-RFV profiles is,
276 as expected, lower than in those profiles where extinction is retrieved above and within
277 the planetary boundary layer. Thus, the figures represent a simple conceptual model of
278 how profiles consisting of all-RFV cases arise with respect to diffuse aerosol backscatter
279 structure and inherently lower signal-to-noise ratios (SNRs). While there are several
280 possible strategies for mitigating this issue for future global satellite lidar missions
281 (discussed in the concluding remarks), the goal for this initial part of the study is to
282 simply depict how the situation is manifested in the base backscatter product measured
283 by the sensor.

284

285 **3.2 Frequency of occurrence for L2 CALIOP all-RFV aerosol profiles**

Atmos. Meas. Tech. Discuss., https://doi.org/10.5194/amt-2017-340
Manuscript under review for journal Atmos. Meas. Tech.
Discussion started: 20 September 2017

Atmospheric Measurement Techniques Discussions

286 The next step of the analysis is to determine the frequency of occurrence of all-
287 RFV profiles in the daytime CALIOP L2_05kmAProf archive. As these data will be
288 collocated with both MODIS and AERONET data for subsequent analysis, no nighttime
289 data are considered here. Table 1 summarizes the statistics of this analysis. For the
290 2010-2011 period, all-RFV profiles make up about 71% (66%) of all daytime CALIOP
291 L2_05kmAProf profiles globally (global oceans-only). However, these statistics include
292 those profiles for which the CALIOP signal was totally attenuated (e.g., by an opaque
293 cloud layer), thus inhibiting aerosol detection near the surface. For context, the 2010-
294 2011 occurrence frequencies of CALIOP not detecting the surface are 39.9% (46.1%)
295 globally (global oceans-only). Roughly 30% of the full archive corresponds with cloud-
296 free conditions (where again, as described in Sec. 2.1, "cloud-free" refers to the
297 implementation of the strictest CALIOP cloud-screening possible where no clouds are
298 classified in the entire profile). Approximately 45% of all cloud-free profiles, and 25%
299 of cloud-free over ocean profiles, are also all-RFV profiles (~15% and 8%, respectively,
300 in absolute terms). The over-ocean sample is next considered below, given the relatively
301 higher fidelity expected in the collocated MODIS AOT data (e.g., Levy et al., 2013).

302 We note that due to the primary CALIOP laser failing in 2009, Table 1 also
303 includes results from a two-year period (2007-2008) before the laser switch to examine
304 any differences in the statistics of the RFV issue between the two lasers. The global
305 frequency of occurrence of all-RFV profiles is consistent for both time periods (i.e.,
306 70.4% for 2007-2008 and 71.1% for 2010-2011), and thus the remainder of this paper
307 focuses on the 2010-2011 analysis alone. We find no evidence to suggest that laser

Atmos. Meas. Tech. Discuss., https://doi.org/10.5194/amt-2017-340
Manuscript under review for journal Atmos. Meas. Tech.
Discussion started: 20 September 2017

performance exhibits any significant influence on the occurrence of per-range bin RFVs and all-RFV profiles within the L2 archive.

The spatial distribution of daytime over-ocean cloud-free all-RFV profiles is shown in Fig. 3. The percentage of cloud-free CALIOP all-RFV aerosol profiles relative to all cloud-free CALIOP aerosol profiles is computed and presented on a 2° x 5° latitude/longitude grid (Fig. 3a). Here we again restrict the analysis to cloud-free scenes to avoid ambiguities in RFV occurrence that are introduced by the presence of clouds. Regions with the largest occurrence frequencies of all-RFV profiles (>75%) include the high latitudes of both the Northern and Southern Hemispheres (NH and SH, respectively). In fact, over snow surfaces, over 80% of CALIOP aerosol profiles are all-RFVs. Over permanent ice (e.g., Greenland), ~99% are all-RFVs. In contrast, the Tropics exhibit the lowest RFV profile occurrence frequencies (<25%). The CALIOP archive contains a significant fraction of all-RFV profiles in polar regions, which is an important result with many ramifications for NASA Earth Observing System science. It is likely that all-RFVs correlate with both low aerosol loading scenarios and high albedo surfaces (e.g., snow and sea ice).

Figure 3 also includes the spatial distribution of mean cloud-free CALIOP-derived AOT (2° x 5° latitude/longitude resolution) without (Fig. 3b) and with (Fig. 3c) all-RFV profiles, demonstrating the quantitative impact of adding all-RFV AOT=0 profiles to the relative analysis. As mentioned above, both approaches have been implemented in past studies. Comparison of the plots reveals that including the all-RFV profiles in the average naturally lowers the mean AOT. To determine the areas for which mean AOTs are most impacted by all-RFVs, the ratio of mean AOT without and with all-

Atmos. Meas. Tech. Discuss., https://doi.org/10.5194/amt-2017-340
Manuscript under review for journal Atmos. Meas. Tech.
Discussion started: 20 September 2017

Atmospheric Measurement Techniques Discussions

331 RFV profiles (i.e., the ratio of Fig. 3b to 3c) is shown in Fig. 3d. Little change in mean
332 AOT is found for most of the oceans, with the exception of the high latitudes of each
333 hemisphere. Overall, global ocean cloud-free mean AOT values of ~0.09 and ~0.07 are
334 found, without and with all-RFV profiles, respectively. Such decrease of mean AOT is
335 expected, as 27% of CALIOP L2 over-ocean cloud-free aerosol profiles are all-RFVs.
336 Also, regions with the largest all-RFV occurrence frequencies (i.e., high latitudes of both
337 the NH and SH) correspond with a greater lowering of mean AOT, compared with those
338 regions (i.e., the Tropics) where small all-RFV occurrence frequencies dominate.
339
340 **3.3 Collocation of MODIS AOT for over-ocean CALIOP all-RFV cases**
341 By collocating MODIS over-ocean AOT retrievals with CALIOP all-RFV
342 profiles, we can estimate the distribution of AOT when algorithm detection/retrieval
343 performance has been compromised. The collocation method applied here is the same as
344 the one used by Toth et al. (2013), where the midpoint of a 10 x 10 km^2 (at nadir) over-
345 ocean MODIS AOT pixel is required to be within 8 km of the temporal midpoint of a 5
346 km L2 CALIOP aerosol profile. Observations outside this range are not considered.
347 After collocation was performed, the number of all cloud-free CALIOP all-RFV profiles
348 were binned by MODIS AOT in 0.01 increments (as depicted in Fig. 4), and separated
349 into three latitude bands: the NH mid-latitudes (30° to 60° N; Fig. 4a), the Tropics (-30°
350 to 30° N; Fig. 4b), and the SH mid-latitudes (-60° to -30° N; Fig. 4c) where coincident
351 data densities are reasonably sufficient. For example, see Fig. 5a for numbers of valid
352 MODIS over-ocean AOT data points available for collocation at 2° x 5°
353 latitude/longitude, based on "Good" or "Very Good" over-ocean L2 MODIS AOT

Atmos. Meas. Tech. Discuss., https://doi.org/10.5194/amt-2017-340
Manuscript under review for journal Atmos. Meas. Tech.
Discussion started: 20 September 2017

retrievals, relative to all corresponding retrievals. For context, Fig. 5b shows the associated spatial distribution of mean L2 MODIS AOT. We note that this includes only those MODIS points collocated with CALIOP, and thus the AOT distributions shown in Fig. 5b are likely different from distributions derived using the full MODIS data record (e.g., Levy et al., 2013).

Modal values of MODIS AOT for all-RFV profiles are found between 0.03 and 0.04, with the exception of the 30° to 60° N band for which the greatest number of all-RFV profiles coincide with MODIS AOTs between 0.04 and 0.05. Thus, the primary mode of CALIOP RFV profiles is 0.03-0.05 from the perspective of MODIS. Corresponding mean and median MODIS AOTs for collocated CALIOP all-RFV profiles are presented in Table 2, with a mean value of 0.07 for the Tropics and NH mid-latitudes, and 0.05 for the SH mid-latitudes band (global mean of 0.06). Median AOTs are similar, though slightly lower, with a global median of 0.05, reflecting the impact of the tail toward higher AOT in the sample distributions. We expect several modes of algorithm response contributing to these distributions, which are borne out in the CALIOP data: layer detection failures due to sensitivity limits, random noise in the attenuated backscatter measurement, and extinction retrieval failures.

While a similar distribution is exhibited for each region, the number of total observations for the Tropics is much greater than that of the other two regions. Thus, the results of Fig. 4b are more robust, which is primarily due to MODIS AOT data availability and collocation (Fig. 5a). Total MODIS occurrence frequencies are greatest in the Tropics (generally >50%), decreasing poleward. The mid-latitude regions exhibit occurrence frequencies less than 25%, with near-zero frequencies observed in the high

Atmos. Meas. Tech. Discuss., https://doi.org/10.5194/amt-2017-340
Manuscript under review for journal Atmos. Meas. Tech.
Discussion started: 20 September 2017

latitudes of the NH and SH. We note the low number of valid MODIS AOT retrievals in the high Northern and Southern latitudes, due at least partly to sea ice extent in these regions (e.g., Ichoku et al., 2003), presents a limitation for our study. That is, the areas for which all-RFV profiles occur most frequently (Fig. 3a) are the same areas with the least numbers of valid MODIS AOT retrievals. Note that in these regions, even for valid MODIS AOT retrievals, biases due to sub-pixel sea ice contamination may still exist.

All-RFV profile occurrence frequencies are computed as a function of MODIS AOT, in order to quantify the amount of CALIOP-derived AOT underestimation at a given MODIS-based AOT. Achieved by division of corresponding data counts in Fig. 4, this underestimation (expressed as a percentage) is shown in line plots in Fig. 6. The same regional sorting and MODIS AOT binning procedures from Fig. 4 are applied. A similar distribution is found for all three latitude bands, with the 0.01-0.02 MODIS AOT bin exhibiting the largest underestimation percentage that gradually lowers toward higher MODIS AOT. CALIOP all-RFV underestimation near 50% is found for the NH and SH mid-latitude regions (Figs. 6a and 6c, respectively) for MODIS AOTs between 0.01 to 0.02, and this value increases to about 70% for the Tropics (Fig. 6b). This implies that 70% of all CALIOP aerosol profiles in this MODIS AOT range are underestimated (i.e., CALIOP reports all-RFV profiles 70% of the time for MODIS AOTs between 0.01 and 0.02).

While the distribution of Fig. 6b is considered most robust, due to MODIS AOT availability in this region, it is important to note that increasingly lower AOTs (i.e., below ~0.03) are within the uncertainty range of MODIS AOT retrievals, and thus these results should be interpreted within the context of this caveat. Also, the relatively low

Atmos. Meas. Tech. Discuss., https://doi.org/10.5194/amt-2017-340
Manuscript under review for journal Atmos. Meas. Tech.
Discussion started: 20 September 2017

400 underestimation percentages corresponding with MODIS AOTs less than 0.02 are
401 believed to be an error, likely resulting from an artifact in the MODIS AOT
402 retrievals/products.
403
404 **3.4 Collocations of CALIOP all-RFV Profiles with AERONET**
405 AERONET data are considered the benchmark for satellite AOT retrievals
406 (Holben et al., 1998). Thus, similar to the over-ocean MODIS analysis above, CALIOP
407 AOT and all-RFV profiles are examined using collocated AOTs derived from
408 measurements collected at coastal and island AERONET sites. Ninety-three sites are
409 used, the locations of which are depicted globally in Fig. 7. Similar to Sec. 3.2, CALIOP
410 L2_05kmAProf data are spatially (within 0.4° latitude/longitude) and temporally (within
411 30 minutes) collocated with Level 2.0 AERONET data. Note that we include all four
412 years (2007-2008 and 2010-2011) for this analysis, as there are far fewer AERONET data
413 points available in contrast to MODIS (e.g., Omar et al., 2013).
414 Figure 8 summarizes the results of the CALIOP/AERONET collocation. In a
415 similar manner as Fig. 4, Fig. 8a is a histogram of the number of cloud-free CALIOP
416 aerosol profiles (all-RFV profiles and all available) for each 0.01 AERONET AOT bin.
417 The overall distribution observed here is comparable to that from MODIS (Fig. 4), but
418 noticeably noisier due to the limited AERONET data sample size. However, peak counts
419 of all-RFV profiles occur for AERONET AOTs between 0.04 and 0.05, which is roughly
420 consistent with the MODIS comparisons. The corresponding mean AERONET AOTs of
421 collocated CALIOP all-RFV profiles are generally higher than those found from MODIS,
422 with values of 0.1 and 0.09 for the Tropics and NH mid-latitudes, respectively (Table 2),

423 and a global mean (median) value of 0.08 (0.07). We note that this analysis may be
424 influenced by residual cloud contamination of subvisible cirrus in the AERONET dataset
425 (e.g., Chew et al., 2011; Huang et al., 2012).

426 Fig. 8b shows all-RFV profile occurrence frequencies as a function of AERONET
427 AOT, computed by dividing the respective counts in Fig. 8a. Again, a noisier overall
428 distribution is found compared with the line plots of Fig. 6. As expected, the 0.01-0.02
429 bin exhibits the largest underestimation percentage. However, while this value is 70%
430 for the MODIS analysis (Fig. 6b), it increases to 100% for AERONET, and we again
431 conclude that an artifact is likely present in the MODIS retrievals for very low aerosol
432 loading cases. While the sample size is small, in the 4-year data set examined in this
433 study, whenever AERONET measured an AOT lower than 0.02 the collocated CALIOP
434 aerosol profiles contained only RFVs.

435

436 **3.5 Reconciling CALIOP AOT Underestimation**

437 In this part of the study, we describe a proof-of-concept analysis that uses one-
438 month of data with the same spatio-temporal domain and conditions introduced in Sec.
439 3.1 to estimate the nominal underestimation of CALIOP AOT due to RFVs in otherwise
440 high-fidelity L2 retrievals (i.e., those where extinction is derived and the profile passes all
441 QA/QC tests). This is achieved by retrieving extinction profiles from the mean global
442 TAB profiles previously constructed from all-RFV profiles (i.e., as presented in Fig. 2).
443 Characterizing these profiles, including those derived for all corresponding/collocated
444 MODIS AOT (Fig. 2a, with an average MODIS AOT of 0.067) and MODIS AOT
445 between 0.03 and 0.07 (Fig. 2c, with an average MODIS AOT of 0.045) to suppress the

446 influence of random algorithm failure events at relatively high AOT, as TAB "noise
447 floors", we then replace RFV bins with corresponding extinction and calculate column-
448 integrated AOT. The premise here assumes that the distribution of aerosol depicted in
449 the TAB noise floors is constant globally. This is highly uncertain, and we strongly
450 caution that the purpose is to provide an initial demonstration of a practical way to
451 correct RFVs in the CALIOP archive.

452 The aerosol extinction profiles for all-RFVs are derived in two steps. First, the
453 top of the surface-attached layer is determined by inspection of the ratio between the
454 measured backscatter and modeled attenuated backscatter, as provided in the CALIPSO
455 L1.5 product. Using a fixed lidar ratio of 29 sr (Kim et al., 2017), an extinction solution
456 is generated from 20 km to the top of the surface-attached layer at 3.5 km (Young and
457 Vaughan, 2009). Integrating this extinction profile provides an estimate of the AOT
458 overlying the surface-attached layer (AOT_{upper}). The derived AOT_{upper} values are ~0.015
459 and ~0.01 for the total all-RFV sample and AOT-limited sample, respectively. These
460 values are not surprising, as they are in agreement with AERONET measurements
461 obtained at the Mauna Loa site (elevation of ~3. 5 km AMSL; Alfaro-Contreras et al.,
462 2016).

463 Next, an extinction solution and optimized estimate of the lidar ratio are
464 generated from 3.5 km to the surface using the AOT of the surface-attached layer; i.e.,
465 AOT_{layer} = column AOT – AOT_{upper}). This step is similar to the above-mentioned
466 approach, except now an iterative process is implemented to derive a lidar ratio for the
467 layer. The lidar ratio is optimized when the integral of the retrieved extinction profile
468 matches AOT_{layer}. Resulting surface-attached layer lidar ratios are 43 sr and 30 sr, for the

469 first and second case respectively, with the latter value comparing reasonably well with
470 the coastal marine lidar ratio of ~28 derived from AERONET analyses (Sayer et al.,
471 2012). However, the lidar ratio solved for the all-RFV sample case is higher than that
472 typical of marine aerosols (i.e., ~26; Dawson et al., 2015), which may be a result of
473 uncertainties in both MODIS and CALIOP datasets. For example, the uncertainty of the
474 lower end of MODIS AOT retrievals is on the order of 0.02-0.03 (Levy et al., 2013).
475 These lidar ratios are also likely biased high due to biases in the daytime CALIOP V3
476 calibration scheme: the V3 daytime calibration coefficients are typically 5% to as much
477 as 30% higher than their V4 counterparts, depending on location and season (Getzewich
478 et al., 2016). Additionally, some all-RFV profiles may include non-marine aerosols,
479 which would further contribute to the high biases in the retrieved lidar ratios.

480 With these caveats in mind, we show the resultant all-RFV extinction profiles in
481 Fig. 9. Extinction coefficients are seen to peak near the surface and decrease
482 exponentially with height. These profiles are thus considered the
483 corresponding/approximated CALIOP extinction-based noise floors. Next, for those
484 cloud-free, over-ocean, L2_05kmAProf CALIOP profiles from the same month
485 (February 2008), the RFV bins within those profiles where some measure of extinction
486 has been observed and passed QA/QC were replaced with the corresponding extinction
487 noise-floor values. Profiles were then reintegrated to yield RFV-corrected AOTs.

488 The results of this exercise are summarized in Table 3. The first result,
489 representing the inclusion of all-RFV profiles as is within bulk global samples (i.e.,
490 adding cases of AOT=0 to a given sample) shows a difference of 0.033 between
491 collocated CALIOP and MODIS AOT. The noise floor correction applied to both all-

492 RFV profiles and those where some extinction was solved yields AOT differences (i.e.,
493 MODIS-CALIOP) of -0.009 and 0.006 depending on the correction sample, which is an
494 improvement (~20% in absolute value) in the agreement of CALIOP and MODIS AOTs.
495 If profiles with nominal extinction are not corrected and all-RFV profiles are ignored, a
496 mean AOT difference of 0.025 is found with MODIS. Applying the noise-floor
497 corrections for this scenario results in AOT differences of -0.013 and 0.001, or a 10-20%
498 improvement (in absolute value) in the disparity in mean AOT between the two sensors.
499 Lastly, we emphasize to the reader that this section describes only an initial attempt to
500 resolve the RFV issue, and can likely be improved in future studies. For example, the
501 noise floor extinction profile is derived using data from global oceans, while a regional
502 dependency is possible. Also, longer spatial and temporal averages of CALIOP data
503 would likely increase the SNRs and reduce the frequency of occurrence of the RFV issue.
504

505 **3.6 Case study: Nighttime CALIOP all-RFV profile occurrence frequencies**

506 The analyses in this paper use daytime CALIOP data to allow for comparison
507 with passively-sensed aerosol observations from MODIS and AERONET. However, for
508 context, in this section we conduct a case study for a two-month (January and February
509 2008) period to investigate the occurrence frequencies of CALIOP all-RFV profiles
510 during nighttime conditions. The same CALIOP products and QA procedures as
511 described earlier are used here, and Table 4 summarizes the results of this analysis.
512 During nighttime, about half of all global CALIOP aerosol profiles for this period are all-
513 RFVs, but this statistic decreases to about 22% when restricted to cloud-free conditions.
514 This percentage lowers even further for over-ocean profiles. Depending on the analysis,

515 absolute decreases between daytime and nighttime all-RFV occurrence frequencies range
516 from ~8% to ~25%. These findings are expected, as the lack of solar background signal
517 during nighttime allows for an increased SNR and improves the ability of the CALIOP
518 algorithms to detect aerosol layers.
519
520 **3.7 Anticipating Version 4 CALIOP Aerosol Products**
521 Version 4 (V4) CALIOP L2 aerosol products were publicly released in
522 November 2016. A case study was thus performed to assess changes in RFV impacts
523 using these new products, again considering cloud-free over-global-ocean observations
524 during daytime conditions. Whereas the broader point of the paper is a conceptualization
525 of the lower-threshold sensitivity of CALIOP to aerosol presence, and the global
526 distribution and impact on overall archive availability, this analysis is included for
527 general consistency. Specifically, V4 data feature improved calibrations of Level 1 (L1)
528 backscatter that may increase the detection sensitivity of diffuse aerosol layers that are
529 reflected in L2 aerosol extinction retrievals, and thus a possible decrease in the
530 occurrence of all-RFV profiles overall.
531 A two-month V4 (January and February of 2008) analysis using QA aerosol
532 profile data (L2_05kmAPro-Standard-V4-10) reveals a 4% relative decrease (1%
533 absolute decrease) in global all-RFV profile occurrence frequencies between V3 and V4.
534 Without QA screening (Sec. 2.1), a 15% relative decrease (2% absolute decrease) is
535 found in the occurrence frequency of all-RFV profiles between versions. A supplemental
536 analysis was also conducted, through the use of the CALIOP aerosol layer product
537 (L2_05kmALay-Standard-V4-10) with alternative cloud screening (i.e., cloud optical

538 depth = 0 instead of the AVD parameter), the results of which are consistent with those
539 from the L2_05kmAPro-Standard-V4-10 test. Though this is an initial look at this
540 important new dataset, it appears that improvements in instrument calibration are likely
541 having some positive influence on retrieval sensitivity, though the broader impact of all-
542 RFV profiles as a limiting factor on the breadth of the CALIOP archive, particularly at
543 the poles, mostly remains.
544
545 **4 Conclusions**
546 Since June 2006, the NASA Cloud-Aerosol Lidar with Orthogonal Polarization
547 (CALIOP) instrument has provided a unique global space-borne view of aerosol vertical
548 distribution in Earth's atmosphere. As indicated by this study, a significant portion of
549 Level 2 (L2) CALIOP 532 nm aerosol profiles consist of retrieval fill values (RFVs)
550 throughout the entire range-resolved column (i.e., all-RFVs), overwhelmingly the result
551 of instrument sensitivity and algorithm layer detection limits. The relevant impact of the
552 all-RFV profile is a subsequent column-integrated aerosol optical thickness (AOT) equal
553 to zero.
554 Using four years (2007-2008 and 2010-2011) of daytime CALIOP Version 3 L2
555 aerosol products, the frequency of occurrence of all-RFV profiles within the CALIOP
556 archive is quantified. L2 retrieval underestimation and lower detectability limits of
557 CALIOP-derived AOT are assessed using collocated L2 aerosol retrievals from over-
558 ocean Aqua Moderate Resolution Imaging Spectroradiometer (MODIS) and
559 coastal/island Aerosol Robotic Network (AERONET) measurements. The results are
560 partitioned into three latitude bands: Northern Hemisphere mid-latitudes (30° to 60° N),

Tropics (-30° to 30° N), and Southern Hemisphere mid-latitudes (-60° to -30° N). The primary findings of this study are:

1. Analysis of CALIOP Level 1.5 attenuated backscatter data reveals that all-RFV profiles are primarily the result of diffuse aerosol layers with inherently lower signal-to-noise ratios (SNRs) that are below CALIOP layer detection limits.
2. All-RFV profiles make up 71% (66%) of all daytime CALIOP L2 aerosol profiles globally (global oceans-only), although this includes completely attenuated columns. For cloud-free CALIOP L2 aerosol profiles, 45% (27%) globally (global oceans-only) are all-RFV profiles. The largest relative all-RFV profile occurrence frequencies (>75%) are found in the high latitudes of both hemispheres, and are smallest (<25%) in the Tropics. The results of this study indicate that there is a significant daytime observational gap in CALIOP aerosol products near the poles, which is a critically important finding for community awareness.
3. The primary mode of CALIOP all-RFV profiles corresponds with MODIS AOTs of 0.03-0.05, which is largely consistent with an AERONET-based analysis. Also, we found that a small fraction of AERONET data have AOTs lower than 0.02, of which all collocated CALIOP L2 profiles are all-RFVs. This finding is consistent with the lowest detectable CALIOP aerosol optical depth range of 0.02-0.04, as hypothesized by Kacenelenbogen et al. (2011).
4. As a preliminary study, aerosol extinction coefficient values for two distinct CALIOP all-RFV profile samples are derived using an inversion algorithm applied to corresponding attenuated backscatter data, and a collection of RFV-

584 corrected mean CALIOP AOTs are estimated for a one-month case study. The
585 mean over-ocean CALIOP AOTs increase 10-20% (in absolute value) after
586 correction, with a closer match to collocated Aqua MODIS mean over-ocean
587 AOT.

588 5. A small decrease in all-RFV profile occurrence is found from Version 4 CALIOP
589 data, which are undergoing widespread release at the time of this writing. Still,
590 the larger-scale impact of all-RFV profiles remains.

591 This research demonstrates that all-RFV profiles exert a significant influence on
592 the L2 CALIOP AOT archive, as these data compose nearly half of global cloud-free
593 CALIOP aerosol points. Disagreements exist in the literature on the manner for which to
594 handle all-RFV profiles when generating Level 3 AOT statistics. Some studies have set
595 the integrated AOTs of all-RFV profiles to zero, for instance, and included them.
596 However, analyses with passive-based sensors presented in this study reveal these AOTs
597 are most certainly non-zero (global mean values of 0.06 for MODIS and 0.08 for
598 AERONET). These findings are not surprising, as this is the baseline AOT range
599 expected under clean maritime conditions (Kaufman et al., 2001; 2005).

600 This research also shows that CALIOP RFVs caused by lower backscatter
601 threshold sensitivities to highly diffuse aerosols, contribute significantly to the
602 discrepancy between CALIOP AOT and those derived from passive sensors like MODIS.
603 Previous studies have mostly attributed this offset to selection of the CALIOP lidar ratio
604 (extinction-to-backscatter ratio) or errors in passive aerosol retrievals. Multi-spectral
605 lidar measurements can begin to close the gap, but will experience SNR issues of their
606 own.

Atmos. Meas. Tech. Discuss., https://doi.org/10.5194/amt-2017-340
Manuscript under review for journal Atmos. Meas. Tech.
Discussion started: 20 September 2017

607 By characterizing lower detection limits of CALIOP-derived extinction and
608 AOT, the potential exists for innovations in instrumentation design and algorithm
609 development of future lidar missions, such as those affiliated with the NASA Aerosol-
610 Clouds-Ecosystems (ACE) mission or the signal processing effort of Mariais et al. (2016).
611 Specifically, increasing the intensity of the lidar signal or implementing larger spatial
612 averaging schemes may help to lower the occurrence frequency of all-RFV profiles and
613 relative RFV occurrence per range bin in L2 products. Questions, however, arise in
614 terms of developing datasets with sufficient spatial and temporal resolution versus needs
615 for optimal data densities, and which is more significant for a given project. Regardless
616 of the potential solution, science teams of current and future lidar systems should
617 carefully consider the existence of RFVs in project datasets.
618
619
620
621
622
623
624
625
626
627
628
629

Acknowledgements

This research was funded with the support of the Office of Naval Research through contract N00014-16-1-2040 (Grant 11843919) and the NASA Earth and Space Science Fellowship program. Authors JZ and TDT acknowledge the support from NASA grant NNX14AJ13G. Author JRC acknowledges the support of the NASA Interagency Agreement IAARPO201422 on behalf of the CALIPSO Science Team. CALIPSO data were obtained from the NASA Langley Research Center Atmospheric Science Data Center (eos-web.larc.nasa.gov). MODIS data were obtained from NASA Goddard Space Flight Center (ladsweb.nascom.nasa.gov). AERONET data were obtained from the project website (aeronet.gsfc.nasa.gov). We acknowledge the AERONET program, and the contributing principal investigators and their staff, for coordinating the sites and data used for this investigation.

References

Alfaro-Contreras, R., Zhang, J., Campbell, J. R., and Reid, J. S.: Investigating the frequency and interannual variability in global above-cloud aerosol characteristics with CALIOP and OMI, Atmospheric Chemistry and Physics, 16(1), 47, 2016.

Campbell, J. R., Reid, J. S., Westphal, D. L., Zhang, J., Hyer, E. J., and Welton, E. J.: CALIOP aerosol subset processing for global aerosol transport model data assimilation, IEEE Journal of Selected Topics in Applied Earth Observations and Remote Sensing, 3(2), 203-214, 2010.

Campbell, J. R. et al.: Evaluating nighttime CALIOP 0.532 μm aerosol optical depth and extinction coefficient retrievals, Atmospheric Measurement Techniques, 5, 2143-2160, doi:10.5194/amt-5-2143-2012, 2012.

Campbell, J. R. et al.: Characterizing the vertical profile of aerosol particle extinction and linear depolarization over Southeast Asia and the Maritime Continent: the 2007-2009 view from CALIOP, Atmos. Res., doi:10.1016/j.atmosres.2012.05.007, 2013.

Chand, D., Wood, R., Anderson, T. L., Satheesh, S. K., and Charlson, R. J.: Satellite-derived direct radiative effect of aerosols dependent on cloud cover, Nature Geoscience, 2(3), 181-184, 2009.

Chew, B. N., Campbell, J. R., Reid, J. S., Giles, D. M., Welton, E. J., Salinas, S. V., and Liew, S. C.: Tropical cirrus cloud contamination in sun photometer data, Atmospheric Environment, 45(37), 6724-6731, 2011.

Dawson, K. W., Meskhidze, N., Josset, D., and Gassó, S.: Spaceborne observations of

the lidar ratio of marine aerosols, Atmos. Chem. Phys., 15, 3241-3255, https://doi.org/10.5194/acp-15-3241-2015, 2015.

Getzewich, B. J., Tackett, J. L, Kar, J., Garnier, A., Vaughan, M. A., and Hunt, B.: CALIOP Calibration: Version 4.0 Algorithm Updates, The 27th International Laser Radar Conference (ILRC 27), EPJ Web of Conferences, 119, 04013, doi:10.1051/epjconf/201611904013, 2016.

Holben, B. N. and coauthors: AERONET - A Federated Instrument Network and Data Archive for Aerosol Characterization, Remote Sens. Environ., 66, 1-16, 1998.

Huang, J. and coauthors: Summer dust aerosols detected from CALIPSO over the Tibetan Plateau, Geophysical Research Letters, 34 (18), 2007.

Huang, J. and coauthors: Evaluations of cirrus contamination and screening in ground aerosol observations using collocated lidar systems, J. Geophys. Res., 117, D15204, doi:10.1029/2012JD017757, 2012.

Ichoku, C., Remer, L. A., Kaufman, Y. J., Levy, R., Chu, D. A., Tanré, D., and Holben, B. N.: MODIS observation of aerosols and estimation of aerosol radiative forcing over southern Africa during SAFARI 2000, Journal of Geophysical Research: Atmospheres, 108(D13), 2003.

Kacenelenbogen, M. and coauthors: An accuracy assessment of the CALIOP/CALIPSO version 2/version 3 daytime aerosol extinction product based on a detailed multi-sensor, multi-platform case study, Atmos. Chem. Phys., 11, 3981–4000, doi:10.5194/acp-11-3981-2011, 2011.

Kanitz, T. and coauthors: Surface matters: limitations of CALIPSO V3 aerosol typing in

698 coastal regions, Atmos. Meas. Tech., 7, 2061-2072, doi:10.5194/amt-7-2061-
699 2014., 2014.
700 Kaufman, Y.J., Smirnov, A., Holben, B. N., and Dubovik, O.: Baseline maritime aerosol:
701 methodology to derive the optical thickness and scattering
702 properties, Geophysical Research Letters, 28(17), pp.3251-3254, 2001.
703 Kaufman, Y. J., Boucher, O., Tanré, D., Chin, M., Remer, L. A., and Takemura, T.:
704 Aerosol anthropogenic component estimated from satellite data, Geophys. Res.
705 Lett., 32, L17804, doi:10.1029/2005GL023125, 2005.
706 Kim, M. H., Kim, S. W., Yoon, S. C., and Omar, A. H.: Comparison of aerosol optical
707 depth between CALIOP and MODIS-Aqua for CALIOP aerosol subtypes over the
708 ocean, Journal of Geophysical Research: Atmospheres, 118*(23)*, 2013.
709 Kim, M. H., Omar, A. H., Vaughan, M. A., Winker, D. M., Trepte, C. R., Hu, Y., Z. Liu,
710 Z., and Kim, S.-W.: Quantifying the low bias of CALIPSO's column aerosol
711 optical depth due to undetected aerosol layers, J. Geophys. Res.
712 Atmos., 122, 1098–1113, doi:10.1002/2016JD025797, 2017.
713 Kittaka, C., Winker, D. M., Vaughan, M. A., Omar, A., and Remer, L. A.:
714 Intercomparison of column aerosol optical depths from CALIPSO and MODIS
715 Aqua, Atmospheric Measurement Techniques, 4(2), 131-141, 2011.
716 Levy, R. C., Mattoo, S., Munchak, L. A., Remer, L. A., Sayer, A. M., Patadia, F., and
717 Hsu, N. C.: The Collection 6 MODIS aerosol products over land and ocean,
718 Atmos. Meas. Tech., 6, 2989-3034, doi:10.5194/amt-6-2989-2013, 2013.
719 Ma, X., Bartlett, K., Harmon, K, and Yu, F.: Comparison of AOD between CALIPSO

and MODIS: significant differences over major dust and biomass burning regions, Atmospheric Measurement Techniques, 6(9), 2391-2401, 2013.

Marais, W., Holz, R. E., Hui, Y. H., Kuehn, R. E., Eloranta, E. E., and Willett, R. M.: Approach to simultaneously denoise and invert backscatter and extinction from photon-limited atmospheric lidar observations, Appl. Opt., 55, 8316-8334, doi: 10.1364/AO.55.008316, 2016.

Martin, R. V.: Satellite remote sensing of surface air quality, Atmospheric Environment, 42(34), 7823-7843, 2008.

Omar, A. H., Won, J. G., Winker, D. M., Yoon, S. C., Dubovik, O., and McCormick, M. P.: Development of global aerosol models using cluster analysis of Aerosol Robotic Network (AERONET) measurements, Journal of Geophysical Research: Atmospheres, 110(D10), 2005.

Omar, A. H. and coauthors: The CALIPSO automated aerosol classification and lidar ratio selection algorithm, Journal of Atmospheric and Oceanic Technology, 26(10), 1994-2014, 2009.

Omar, A. H. and coauthors: CALIOP and AERONET aerosol optical depth comparisons: One size fits none, Journal of Geophysical Research: Atmospheres, 118, 4748–4766, doi:10.1002/jgrd.50330, 2013.

Prados, A. I., Leptoukh, G., Lynnes, C., Johnson, J., Rui, H., Chen, A., and Husar, R. B.: Access, visualization, and interoperability of air quality remote sensing data sets via the Giovanni online tool, IEEE Journal of Selected Topics in Applied Earth Observations and Remote Sensing, 3(3), 359-370, 2010.

Redemann, J. and coauthors: The comparison of MODIS-Aqua (C5) and CALIOP (V2 &

743 V3) aerosol optical depth, Atmos. Chem. Phys., 12, 3025-3043, doi:10.5194/acp-
744 12-3025-2012, 2012.
745 Reid, J. S., and coauthors: Ground-based High Spectral Resolution Lidar observation of
746 aerosol vertical distribution in the summertime Southeast United States, J.
747 Geophys. Res. Atmos., 122, 2970–3004, doi:10.1002/2016JD025798, 2017.
748 Rogers, R. R. and coauthors: Looking through the haze: evaluating the CALIPSO level 2
749 aerosol optical depth using airborne high spectral resolution lidar data,
750 Atmospheric Measurement Techniques, 7(12), 4317-4340, 2014.
751 Sayer, A. M., Smirnov, A., Hsu, N. C., and Holben, B. N.: A pure marine aerosol model, for
752 use in remote sensing applications, J. Geophys. Res., 117, D05213,
753 doi:10.1029/2011JD016689, 2012.
754 Schuster, G. L. and coauthors: Comparison of CALIPSO aerosol optical depth retrievals
755 to AERONET measurements, and a climatology for the lidar ratio of dust, Atmos.
756 Chem. Phys., 12(16), 7431-7452, 2012.
757 Sekiyama, T. T., Tanaka, T. Y., Shimizu, A., and Miyoshi, T.: Data assimilation of
758 CALIPSO aerosol observations, Atmospheric Chemistry and Physics, 10(1), 39-
759 49, 2010.
760 Shi, Y., Zhang, J., Reid, J. S., Hyer, E. J., Eck, T. F., Holben, B. N., and Kahn, R. A.: A
761 critical examination of spatial biases between MODIS and MISR aerosol products
762 - application for potential AERONET deployment, Atmospheric Measurement
763 Techniques, Vol. 4, No. 12, 2823-2836, doi: 10.5194/amt-4-2823-2011, 2011.
764 Smirnov, A. and coauthors: Maritime aerosol network as a component of AERONET –
765 first results and comparison with global aerosol models and satellite retrievals,
766 Atmos. Meas. Tech., 4, 583-597, doi:10.5194/amt-4-583-2011, 2011.

767 Stephens, G. L. and coauthors: The CloudSat mission and the A-Train: A new dimension
768 of space-based observations of clouds and precipitation, Bulletin of the American
769 Meteorological Society, 83(12), 1771-1790, 2002.
770 Thorsen, T. J. and Fu, Q.: CALIPSO-inferred aerosol direct radiative effects: Bias
771 estimates using ground-based Raman lidars, J. Geophys. Res. Atmos., 120, 12,
772 209–12, 220, doi:10.1002/2015JD024095, 2015.
773 Toth, T. D. and coauthors: Investigating enhanced Aqua MODIS aerosol optical depth
774 retrievals over the mid-to-high latitude Southern Oceans through intercomparison
775 with co-located CALIOP, MAN, and AERONET data sets, Journal of
776 Geophysical Research: Atmospheres, 118(10), 4700-4714, 2013.
777 Toth, T. D., Zhang, J., Campbell, J. R., Hyer, E. J., Reid, J. S., Shi, Y., and Westphal, D.
778 L.: Impact of data quality and surface-to-column representativeness on the
779 PM2.5/satellite AOT relationship for the contiguous United States, Atmospheric
780 Chemistry and Physics, 14(12), 6049-6062, 2014.
781 Toth, T. D., Zhang, J., Campbell, J. R., Reid, J. S., and Vaughan, M. A.: Temporal
782 variability of aerosol optical thickness vertical distribution observed from
783 CALIOP, Journal of Geophysical Research: Atmospheres, 121(15), 9117-9139,
784 2016.
785 Vaughan, M. A. and coauthors: Fully automated detection of cloud and aerosol layers in
786 the CALIPSO lidar measurements, J. Atmos. Ocean. Tech., 26, 2034–2050, 2009.
787 Vaughan, M. and coauthors: Adapting CALIPSO Climate Measurements for Near Real
788 Time Analyses and Forecasting, in: Proceedings of the 34th International
789 Symposium on Remote Sensing of Environment, 10–15 April 2011, Sydney,

790 Australia, http://www
791 calipso.larc.nasa.gov/resources/pdfs/VaughanM_211104015final00251.pdf, 2011.
792 Winker, D. M. and coauthors: Overview of the CALIPSO Mission and CALIOP Data
793 Processing Algorithms, J. Atmos. Oceanic Technol., 26, 2310–2323, 2009.
794 Winker, D. M. and coauthors: The CALIPSO mission: A global 3D view of aerosols and
795 clouds, Bulletin of the American Meteorological Society, 91(9), 1211, 2010.
796 Winker, D. M., Tackett, J. L, Getzewich, B. J., Liu, Z., Vaughan, M. A., and Rogers, R.
797 R.: The global 3-D distribution of tropospheric aerosols as characterized by
798 CALIOP, Atmospheric Chemistry and Physics, 13, 3345-3361, doi:10.5194/acp-
799 13 3345-2013, 2013.
800 Young, S. A. and Vaughan, M. A.: The retrieval of profiles of particulate extinction from
801 Cloud Aerosol Lidar Infrared Pathfinder Satellite Observations (CALIPSO) data:
802 Algorithm description, J. Atmos. Oceanic Technol., 26, 1105–1119,
803 doi:10.1175/2008JTECHA1221.1, 2009.
804 Yu, H., Chin, M., Winker, D. M., Omar, A. H., Liu, Z., Kittaka, C., and Diehl, T.: Global
805 view of aerosol vertical distributions from CALIPSO lidar measurements and
806 GOCART simulations: Regional and seasonal variations, Journal of Geophysical
807 Research: Atmospheres (1984–2012), 115 (D4), 2010.
808 Zhang, J., Campbell, J. R., Hyer, E. J., Reid, J. S., Westphal, D. L., and Johnson, R. S.:
809 Evaluating the impact of multisensory data assimilation on a global aerosol
810 particle transport model, J. Geophys. Res. Atmos., 119, 4674–4689,
811 doi:10.1002/2013JD020975, 2014.
812 Zhang, J., Campbell, J. R., Reid, J. S., Westphal, D. L., Baker, N. L., Campbell, W. F.,

and Hyer, E. J.: Evaluating the impact of assimilating CALIOP-derived aerosol extinction profiles on a global mass transport model, Geophysical Research Letters, 38(14), 2011.

836 **Figure and Table Captions**
837
838 Figure 1: For data collected during daytime on July 2nd, 2010 over the Arctic, browse
839 image curtain plots of CALIPSO (a) 532 nm total attenuated backscatter (km^{-1} sr^{-1}) and
840 (b) corresponding vertical feature mask (VFM). The white box represents an example
841 segment of the granule for which range bins in the associated Level 2 (L2) aerosol
842 extinction coefficient profile are all retrieval fill values (RFVs), as the VFM classified
843 these bins as either surface (green) or clear air (blue) features. The white arrow indicates
844 a column in which some aerosol has been detected (orange), and the resultant L2 aerosol
845 extinction profile for this column is shown in (c).
846
847 Figure 2: For February 2008, mean profiles of (a, c) Level 1.5 total attenuated
848 backscatter (TAB) and (b, d) attenuated scattering ratio (TAB/molecular attenuated
849 backscatter) over global oceans, corresponding to Level 2 all-RFV (in blue) and non-all-
850 RFV (AOT > 0; in red) profiles. The left column is from an analysis of all cloud-free
851 CALIOP points over global oceans and the right column represents only those collocated
852 with MODIS AOTs between 0.03 and 0.07.
853
854 Figure 3: For 2010-2011, (a) the frequency of occurrence (%) of cloud-free CALIOP
855 profiles at 2° x 5° latitude/longitude grid spacing. Also shown are the corresponding
856 cloud-free mean CALIOP column AOTs (b) without and (c) with all-RFV profiles, and
857 (d) the ratio of (b) to (c).
858

859 Figure 4: For 2010-2011, histograms of all over-ocean cloud-free CALIOP profiles (in
860 green) and all-RFV profiles (in purple) as a function of collocated Aqua MODIS AOT
861 (0.01 bins), for (a) 30° to 60° N, (b) -30° to 30° N, and (c) -60° to -30° N.
862
863 Figure 5: For 2010-2011, (a) frequency of occurrence (%) of valid ("Good" or "Very
864 Good") over-ocean Level 2 (L2) MODIS AOT retrievals, relative to all over-ocean L2
865 MODIS AOT retrievals, for every 2° x 5° latitude/longitude grid box. Also shown is (b)
866 the corresponding spatial distribution of mean L2 MODIS AOT for the same time period.
867 This analysis includes only those MODIS points collocated with CALIOP.
868
869 Figure 6: 2010-2011 frequency of occurrence (%) of over-ocean cloud-free CALIOP all-
870 RFV profiles, relative to all cloud-free CALIOP profiles, as a function of collocated
871 Aqua MODIS AOT (0.01 bins), for (a) 30° to 60° N, (b) -30° to 30° N, and (c) -60° to -
872 30° N.
873
874 Figure 7: Map of the ninety-three coastal/island AERONET sites with Level 2.0 data, for
875 the 2007-2008 and 2010-2011 periods, used for collocation with over-ocean CALIOP
876 aerosol observations.
877
878 Figure 8: For the 2007-2008 and 2010-2011 periods, (a) histograms of all cloud-free
879 CALIOP profiles (in green) and all-RFV profiles (in purple), and (b) corresponding
880 frequency of occurrence (%) of cloud-free CALIOP all-RFV profiles, relative to all
881 cloud-free CALIOP profiles, both as a function of collocated coastal/island AERONET
882 AOT (0.01 bins).

883

884 Figure 9: For February 2008 over cloud-free global oceans, the all-RFV aerosol
885 extinction coefficient profiles derived from the inversion algorithm. The black curve
886 represents all cloud-free CALIOP profiles over global oceans, while the green curve is
887 from an analysis restricted to only those CALIOP points collocated with MODIS AOTs
888 between 0.03 and 0.07.

889

890 Table 1: Statistical summary of the results for this study, for the 2007-2008 and 2010-
891 2011 periods, both globally and for global oceans only. The values in bold and
892 parentheses represent the percentages of each category relative to the entire CALIOP
893 aerosol profile archive for each respective period.

894

895 Table 2: Mean and median values of AOTs derived from Aqua MODIS (2010-2011) and
896 AERONET (2007-2008; 2010-2011), both independently collocated with CALIOP all-
897 RFV profiles.

898

899 Table 3: For February 2008 over cloud-free global oceans, mean values of collocated
900 CALIOP and MODIS AOTs for various scenarios related to the treatment of non-all-RFV
901 and all-RFV CALIOP aerosol profiles. For those scenarios that involve correction, [1]
902 refers to analyses including all cloud-free CALIOP profiles over global oceans, while [2]
903 refers to analyses restricted to CALIOP points collocated with MODIS AOTs between
904 0.03 and 0.07. The corresponding aerosol extinction profiles used for RFV correction are
905 shown in Fig. 9.

Atmos. Meas. Tech. Discuss., https://doi.org/10.5194/amt-2017-340
Manuscript under review for journal Atmos. Meas. Tech.
Discussion started: 20 September 2017

Atmospheric Measurement Techniques Discussions

Table 4: All-RFV CALIOP occurrence frequencies for two months (January and February 2008) from various analyses using daytime and nighttime data, as well as their corresponding absolute differences.

Atmos. Meas. Tech. Discuss., https://doi.org/10.5194/amt-2017-340
Manuscript under review for journal Atmos. Meas. Tech.
Discussion started: 20 September 2017

Atmospheric Measurement Techniques Discussions

948 **Figures**
949

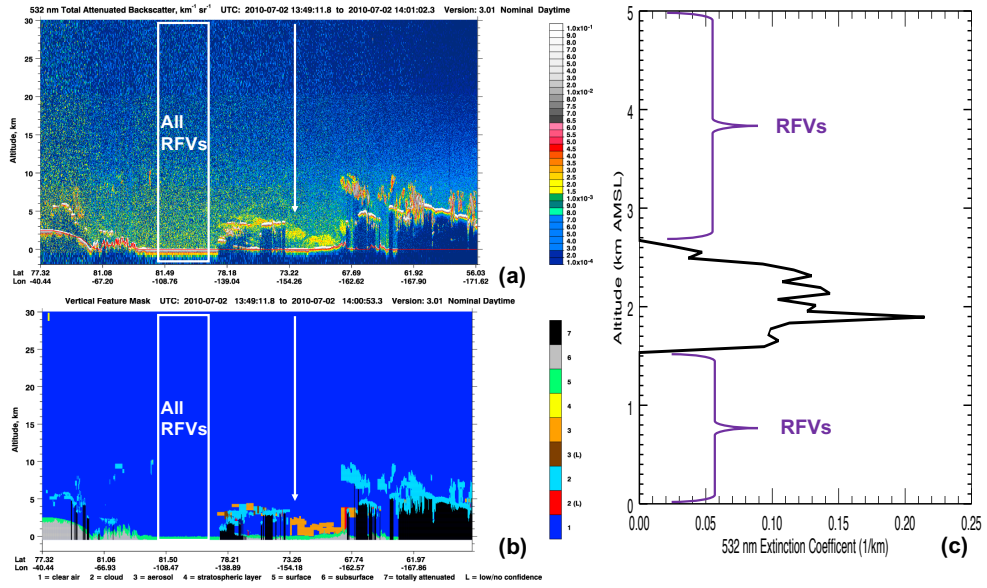

Figure 1: For data collected during daytime on July 2nd, 2010 over the Arctic, browse image curtain plots of CALIPSO (a) 532 nm total attenuated backscatter (km^{-1} sr^{-1}) and (b) corresponding vertical feature mask (VFM). The white box represents an example segment of the granule for which range bins in the associated Level 2 (L2) aerosol extinction coefficient profile are all retrieval fill values (RFVs), as the VFM classified these bins as either surface (green) or clear air (blue) features. The white arrow indicates a column in which some aerosol has been detected (orange), and the resultant L2 aerosol extinction profile for this column is shown in (c).

950
951
952
953
954
955
956
957
958

Atmos. Meas. Tech. Discuss., https://doi.org/10.5194/amt-2017-340
Manuscript under review for journal Atmos. Meas. Tech.
Discussion started: 20 September 2017

Atmospheric Measurement Techniques Discussions

959

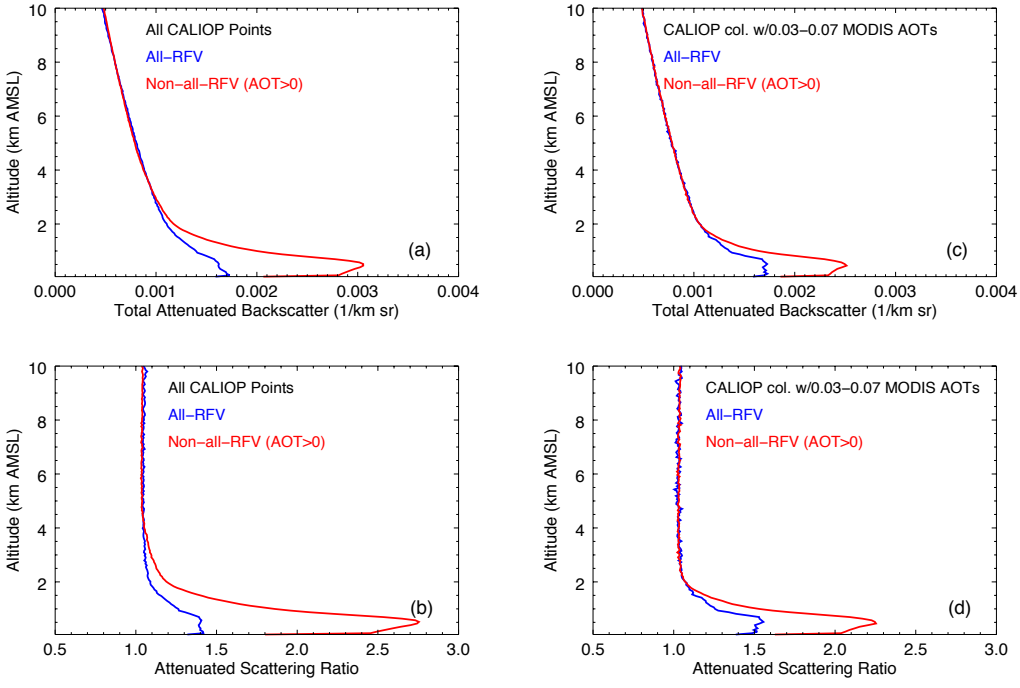

Figure 2: For February 2008, mean profiles of (a, c) Level 1.5 total attenuated backscatter (TAB) and (b, d) attenuated scattering ratio (TAB/molecular attenuated backscatter) over global oceans, corresponding to Level 2 all-RFV (in blue) and non-all-RFV (AOT > 0; in red) profiles. The left column is from an analysis of all cloud-free CALIOP points over global oceans and the right column represents only those collocated with MODIS AOTs between 0.03 and 0.07.

960
961
962
963

Atmos. Meas. Tech. Discuss., https://doi.org/10.5194/amt-2017-340
Manuscript under review for journal Atmos. Meas. Tech.
Discussion started: 20 September 2017

Atmospheric Measurement Techniques Discussions

964

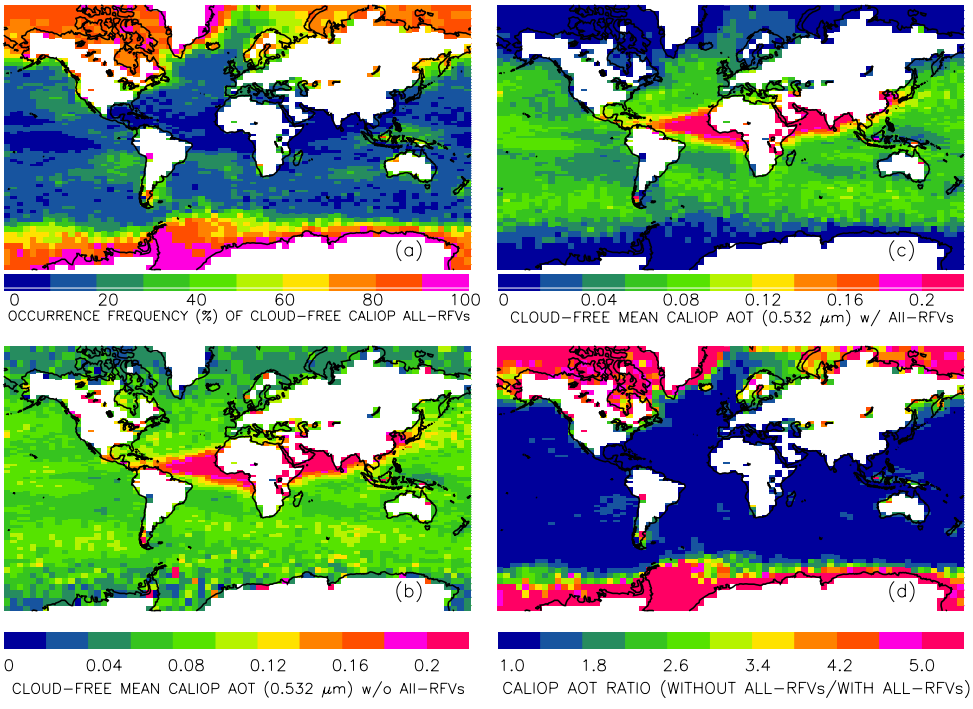

Figure 3: For 2010-2011, (a) the frequency of occurrence (%) of cloud-free CALIOP profiles at 2° x 5° latitude/longitude grid spacing. Also shown are the corresponding cloud-free mean CALIOP column AOTs (b) without and (c) with all-RFV profiles, and (d) the ratio of (b) to (c).

965
966

Atmos. Meas. Tech. Discuss., https://doi.org/10.5194/amt-2017-340
Manuscript under review for journal Atmos. Meas. Tech.
Discussion started: 20 September 2017

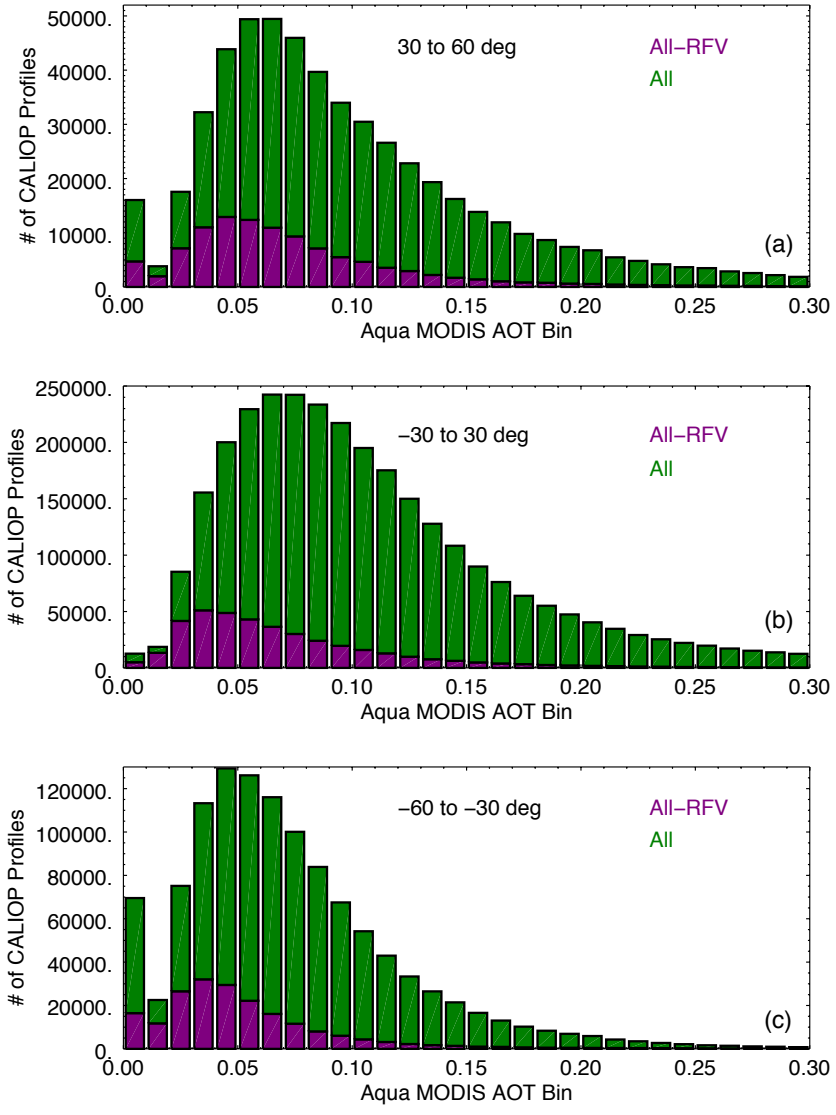

Figure 4: For 2010-2011, histograms of all over-ocean cloud-free CALIOP profiles (in green) and all-RFV profiles (in purple) as a function of collocated Aqua MODIS AOT (0.01 bins), for (a) 30° to 60° N, (b) -30° to 30° N, and (c) -60° to -30° N.

967
968

Atmos. Meas. Tech. Discuss., https://doi.org/10.5194/amt-2017-340
Manuscript under review for journal Atmos. Meas. Tech.
Discussion started: 20 September 2017

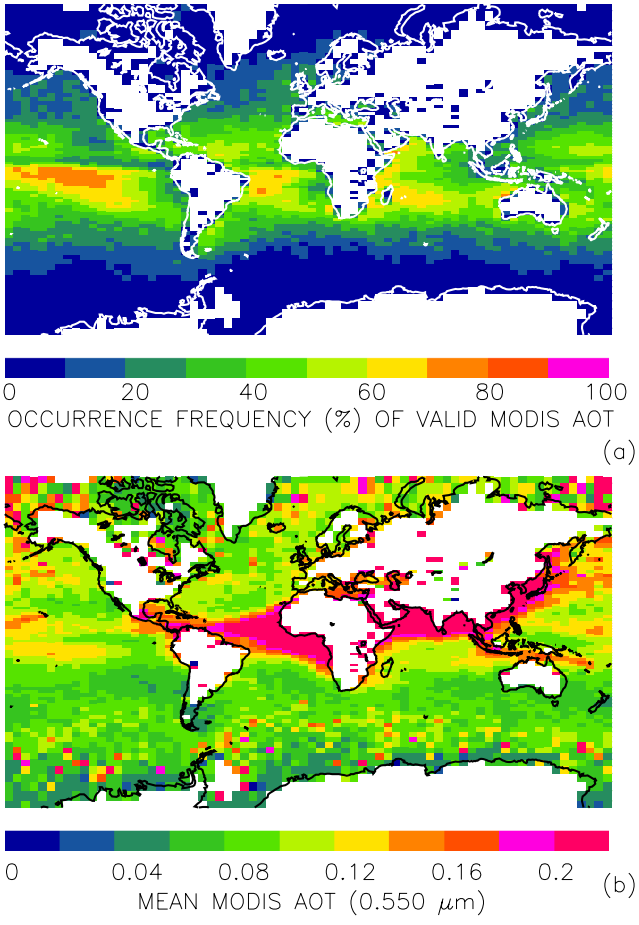

Figure 5: For 2010-2011, (a) frequency of occurrence (%) of valid ("Good" or "Very Good") over-ocean Level 2 (L2) MODIS AOT retrievals, relative to all over-ocean L2 MODIS AOT retrievals, for every 2° x 5° latitude/longitude grid box. Also shown is (b) the corresponding spatial distribution of mean L2 MODIS AOT for the same time period. This analysis includes only those MODIS points collocated with CALIOP.

Atmos. Meas. Tech. Discuss., https://doi.org/10.5194/amt-2017-340
Manuscript under review for journal Atmos. Meas. Tech.
Discussion started: 20 September 2017

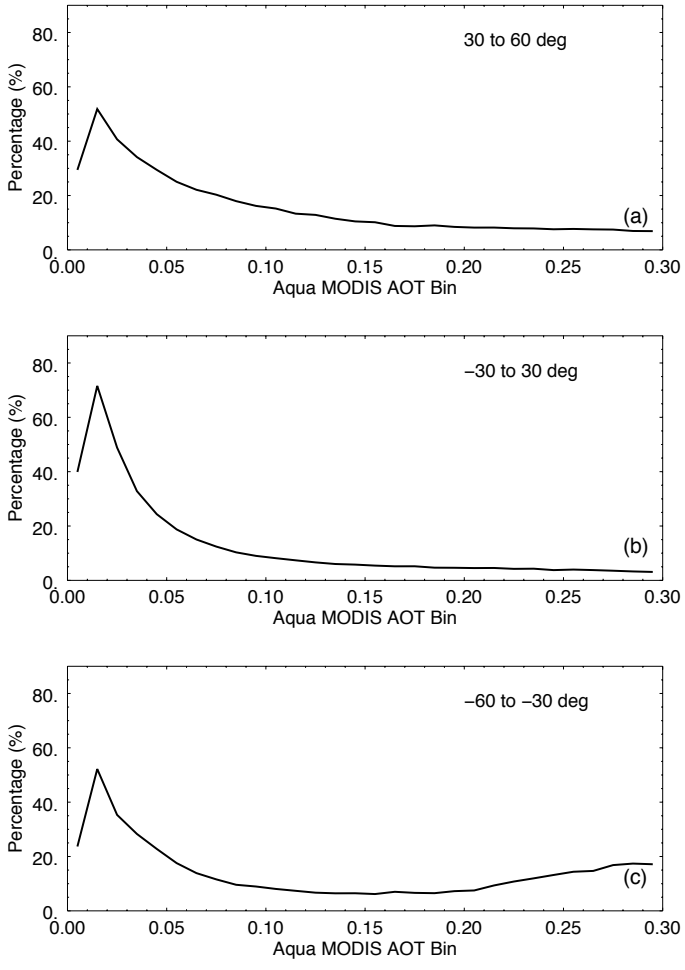

Figure 6: 2010-2011 frequency of occurrence (%) of over-ocean cloud-free CALIOP all-RFV profiles, relative to all cloud-free CALIOP profiles, as a function of collocated Aqua MODIS AOT (0.01 bins), for (a) 30° to 60° N, (b) -30° to 30° N, and (c) -60° to -30° N.

Atmos. Meas. Tech. Discuss., https://doi.org/10.5194/amt-2017-340
Manuscript under review for journal Atmos. Meas. Tech.
Discussion started: 20 September 2017

Atmospheric Measurement Techniques Discussions

981

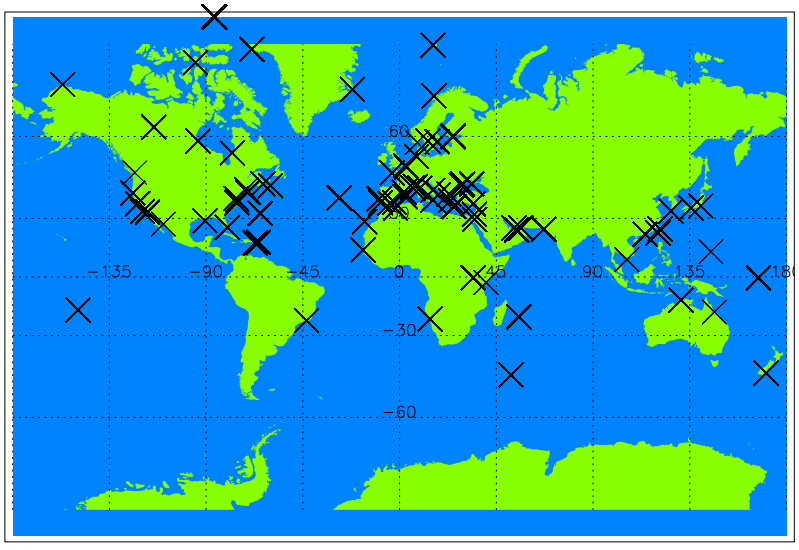

Figure 7: Map of the ninety-three coastal/island AERONET sites with Level 2.0 data, for the 2007-2008 and 2010-2011 periods, used for collocation with over-ocean CALIOP aerosol observations.

982
983
984
985
986
987
988
989
990
991
992
993
994
995
996

Atmos. Meas. Tech. Discuss., https://doi.org/10.5194/amt-2017-340
Manuscript under review for journal Atmos. Meas. Tech.
Discussion started: 20 September 2017

Atmospheric Measurement Techniques Discussions

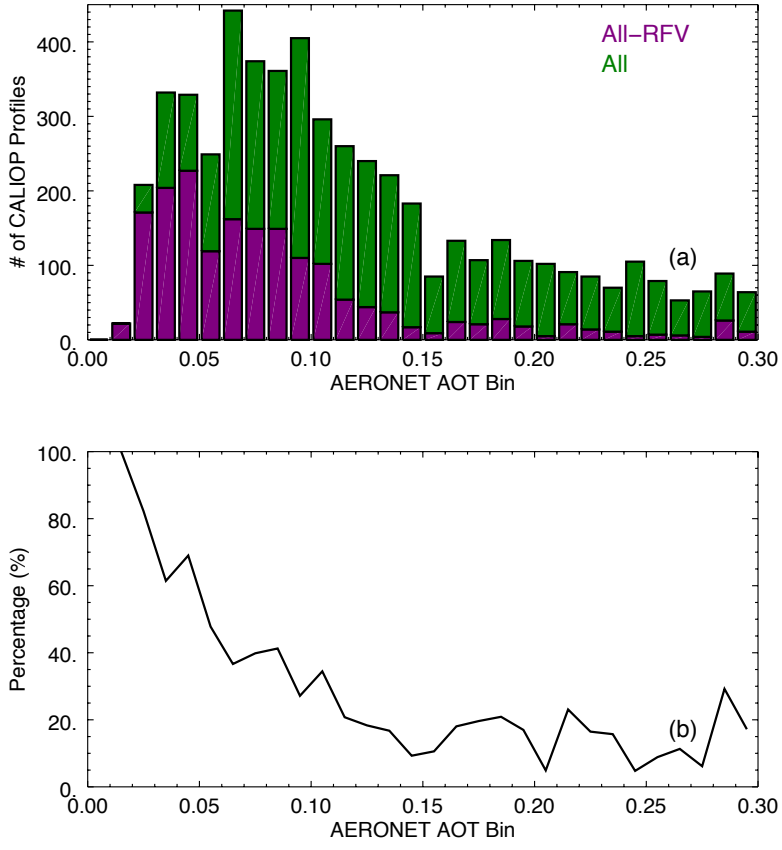

Figure 8: For the 2007-2008 and 2010-2011 periods, (a) histograms of all cloud-free CALIOP profiles (in green) and all-RFV profiles (in purple), and (b) corresponding frequency of occurrence (%) of cloud-free CALIOP all-RFV profiles, relative to all cloud-free CALIOP profiles, both as a function of collocated coastal/island AERONET AOT (0.01 bins).

997
998
999
1000
1001
1002
1003
1004
1005

Atmos. Meas. Tech. Discuss., https://doi.org/10.5194/amt-2017-340
Manuscript under review for journal Atmos. Meas. Tech.
Discussion started: 20 September 2017

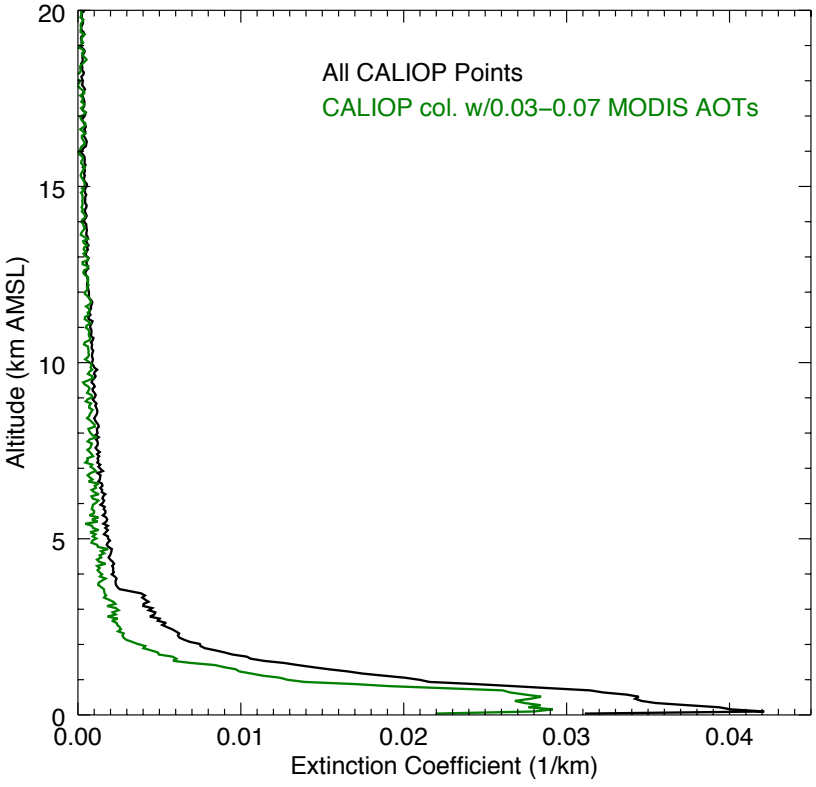

Figure 9: For February 2008 over cloud-free global oceans, the all-RFV aerosol extinction coefficient profiles derived from the inversion algorithm. The black curve represents all cloud-free CALIOP profiles over global oceans, while the green curve is from an analysis restricted to only those CALIOP points collocated with MODIS AOTs between 0.03 and 0.07.

Atmos. Meas. Tech. Discuss., https://doi.org/10.5194/amt-2017-340
Manuscript under review for journal Atmos. Meas. Tech.
Discussion started: 20 September 2017

Atmospheric Measurement Techniques Discussions

1015
1016
1017 **TABLES**
1018
1019
1020

Number of 5 km CALIOP Profiles	Globe		Global Oceans	
	2007-2008	**2010-2011**	**2007-2008**	**2010-2011**
Total	41,929,328	41,188,208	27,742,947	27,198,000
All-RFV	29,503,781 (**70.4%**)	29,297,919 (**71.1%**)	18,190,188 (**65.6%**)	18,026,930 (**66.3%**)
Cloud-free	13,317,918 (**31.8%**)	13,190,530 (**32.0%**)	8,006,719 (**28.9%**)	7,812,682 (**28.7%**)
Cloud-free & all-RFV	5,764,098 (**13.7%**)	5,899,221 (**14.3%**)	2,089,865 (**7.5%**)	2,101,155 (**7.7%**)
Cloud-free, all-RFV, & MODIS AOT≥0	791,570 (**1.9%**)	814,514 (**2.0%**)	781,983 (**2.8%**)	803,546 (**3.0%**)

Table 1: Statistical summary of the results for this study, for the 2007-2008 and 2010-2011 periods, both globally and for global oceans only. The values in bold and parentheses represent the percentages of each category relative to the entire CALIOP aerosol profile archive for each respective period.

1021
1022

Atmos. Meas. Tech. Discuss., https://doi.org/10.5194/amt-2017-340
Manuscript under review for journal Atmos. Meas. Tech.
Discussion started: 20 September 2017

Atmospheric Measurement Techniques Discussions

1023
1024
1025
1026

Region	MODIS		AERONET	
	Mean	Median	Mean	Median
90°S to 60°S	0.05	0.04	-	-
60°S to 30°S	0.05	0.04	0.04	0.04
30°S to 30°N	0.07	0.06	0.1	0.1
30°N to 60°N	0.07	0.06	0.09	0.08
60°N to 90°N	0.07	0.06	0.05	0.04
Globe	0.06	0.05	0.08	0.07

Table 2: Mean and median values of AOTs derived from Aqua MODIS (2010-2011) and AERONET (2007-2008; 2010-2011), both independently collocated with CALIOP all-RFV profiles.

1027
1028
1029

Atmos. Meas. Tech. Discuss., https://doi.org/10.5194/amt-2017-340
Manuscript under review for journal Atmos. Meas. Tech.
Discussion started: 20 September 2017

Atmospheric Measurement Techniques Discussions

Scenario	Mean AOT		
	CALIOP	MODIS	ΔAOT (MODIS-CALIOP)
Uncorrected non-all-RFVs; all-RFVs set to zero	0.084	0.117	0.033
Corrected non-all-RFVs; corrected all-RFVs [1]	0.126	0.117	-0.009
Corrected non-all-RFVs; corrected all-RFVs [2]	0.111	0.117	0.006
Uncorrected non-all-RFVs; all-RFVs ignored	0.098	0.123	0.025
Corrected non-all-RFVs; all-RFVs ignored [1]	0.136	0.123	-0.013
Corrected non-all-RFVs; all-RFVs ignored [2]	0.122	0.123	0.001

Table 3: For February 2008 over cloud-free global oceans, mean values of collocated CALIOP and MODIS AOTs for various scenarios related to the treatment of non-all-RFV and all-RFV CALIOP aerosol profiles. For those scenarios that involve correction, [1] refers to analyses including all cloud-free CALIOP profiles over global oceans, while [2] refers to analyses restricted to CALIOP points collocated with MODIS AOTs between 0.03 and 0.07. The corresponding aerosol extinction profiles used for RFV correction are shown in Fig. 9.

Atmos. Meas. Tech. Discuss., https://doi.org/10.5194/amt-2017-340
Manuscript under review for journal Atmos. Meas. Tech.
Discussion started: 20 September 2017

Atmospheric Measurement Techniques Discussions

Analysis		All Points	Cloud-free
Daytime	Globe	70.7%	46.7%
	Global Oceans	63.4%	21.8%
Nighttime	Globe	53.5%	22.0%
	Global Oceans	52.2%	14.0%
Nighttime - Daytime	Globe	-17.2%	-24.7%
	Global Oceans	-11.2%	-7.8%

Table 4: All-RFV CALIOP occurrence frequencies for two months (January and February 2008) from various analyses using daytime and nighttime data, as well as their corresponding absolute differences.